

## A bio-optical algorithm for the remote estimation of the chlorophyll-a concentration in case 2 waters

This article has been downloaded from IOPscience. Please scroll down to see the full text article.

2009 Environ. Res. Lett. 4 045003

(<http://iopscience.iop.org/1748-9326/4/4/045003>)

View [the table of contents for this issue](#), or go to the [journal homepage](#) for more

Download details:

IP Address: 38.107.179.211

The article was downloaded on 21/02/2012 at 19:31

Please note that [terms and conditions apply](#).

# A bio-optical algorithm for the remote estimation of the chlorophyll-*a* concentration in case 2 waters

Anatoly A Gitelson, Daniela Gurlin, Wesley J Moses and Tadd Barrow

Center for Advanced Land Management Information Technologies (CALMIT),  
School of Natural Resources, University of Nebraska-Lincoln, USA

E-mail: [agitelson2@unl.edu](mailto:agitelson2@unl.edu)

Received 25 February 2009

Accepted for publication 14 May 2009

Published 15 October 2009

Online at [stacks.iop.org/ERL/4/045003](http://stacks.iop.org/ERL/4/045003)

## Abstract

The objective of this work was to test the performance of a recently developed three-band model and its special case, a two-band model, for the remote estimation of the chlorophyll-*a* (chl-*a*) concentration in turbid productive case 2 waters. We specifically focused on (a) determining the ability of the models to estimate chl-*a* < 20 mg m<sup>-3</sup>, typical for coastal and estuarine waters, and (b) assessing the potential of MODIS and MERIS to estimate chl-*a* concentrations in turbid productive waters, using red and near-infrared (NIR) bands. Reflectance spectra and water samples were collected in 89 stations over lakes in the United States with a wide variability in optical parameters (i.e. 2.1 < chl-*a* < 184 mg m<sup>-3</sup>; 0.5 < Secchi disk depth < 4.2 m; 1.2 < total suspended matter < 15 mg l<sup>-1</sup>). The three-band model, using wavebands around 670, 710 and 750 nm, explains more than 89% of the chl-*a* variation for chl-*a* ranging from 2 to 20 mg m<sup>-3</sup> and can be used to estimate chlorophyll-*a* concentrations with a root mean square error (RMSE) of <1.65 mg m<sup>-3</sup>. MODIS (bands 13 and 15) and MERIS (bands 7, 9, and 10) red and NIR reflectances were simulated from the collected reflectance spectra and potential estimation errors were assessed. The MODIS two-band model is able to estimate chl-*a* concentrations with a RMSE of <7.5 mg m<sup>-3</sup> for chl-*a* ranging from 2 to 50 mg m<sup>-3</sup>; however, the model loses its sensitivity for chl-*a* < 20 mg m<sup>-3</sup>. Benefiting from the higher spectral resolution of the MERIS data, the MERIS three-band model accounts for 93% of chl-*a* variation and is able to estimate chl-*a* concentrations with a RMSE of <5.1 mg m<sup>-3</sup> for chl-*a* ranging from 2 to 50 mg m<sup>-3</sup>, and a RMSE of <1.7 mg m<sup>-3</sup> for chl-*a* ranging from 2 to 20 mg m<sup>-3</sup>. These findings imply that, provided that an atmospheric correction scheme specific to the red and NIR spectral region is available, the extensive database of MODIS and MERIS images could be used to quantitatively monitor chl-*a* in case 2 waters.

**Keywords:** remote estimation, reflectance, chl-*a* concentration, case 2 waters

## 1. Introduction

Remote estimation of the concentrations of water constituents is based on the relationship between the remote-sensing reflectance,  $R_{rs}(\lambda)$ , and the inherent optical properties, backscattering coefficient,  $b_b(\lambda)$ , and absorption coefficient,  $a(\lambda)$ :

$$R_{rs}(\lambda) \propto \frac{b_b(\lambda)}{a(\lambda) + b_b(\lambda)} \quad (1)$$

where  $a(\lambda)$  is the sum of the absorption coefficients of phytoplankton pigments,  $a_{\text{pigm}}$ , coloured dissolved organic matter,  $a_{\text{CDOM}}$ , non-algal particles,  $a_{\text{NAP}}$ , and pure water,  $a_{\text{water}}$  (e.g., Gordon *et al* 1988).

To retrieve the chl-*a* concentration from spectral reflectance, one has to isolate the chl-*a* absorption coefficient. In open ocean waters chl-*a* is derived using the blue and green spectral regions (e.g., Gordon and Morel 1983). However, in turbid productive case 2 waters, these spectral regions

cannot be used to estimate chl-*a* because of the overlapping, uncorrelated absorptions by CDOM and NAP, which are much larger in these waters (e.g., GKSS 1986, Gitelson 1992, Gons 1999, Dall'Olmo *et al* 2005).

Algorithms developed for estimating chl-*a* in turbid productive waters are based on the properties of the reflectance peak near 700 nm (e.g., Vasilkov and Kopelevich 1982, Gitelson *et al* 1985, Stumpf and Tyler 1988, Gitelson 1992, Gons 1999, Gower *et al* 1999). Recently, Dall'Olmo and Gitelson (2005) provided evidence that a three-band reflectance model, originally developed for estimating pigment contents in terrestrial vegetation (Gitelson *et al* 2003, 2005), could also be used to assess chl-*a* in turbid productive waters. The model relates pigment concentration  $C_{\text{pig}}^{\text{m}}$  to reflectance  $R(\lambda_i)$  in three spectral bands  $\lambda_i$  (Gitelson *et al* 2003):

$$C_{\text{pig}}^{\text{m}} \propto [R^{-1}(\lambda_1) - R^{-1}(\lambda_2)] \times R(\lambda_3). \quad (2)$$

It was shown that for estimating chl-*a*,  $\lambda_1$  should be in the red range around 670 nm,  $\lambda_2$  in the range around 710 nm and  $\lambda_3$  in the NIR range around 750 nm (Dall'Olmo and Gitelson 2006, Gitelson *et al* 2007, 2008).

The three-band model (equation (2)) was tested using observations from lakes with variable optical properties (Dall'Olmo and Gitelson 2005, Gitelson *et al* 2008) as well as in estuarine waters (Gitelson *et al* 2007, 2008). In these studies chl-*a* varied widely, reaching as high as hundreds of  $\text{mg m}^{-3}$ , which is typical for hypereutrophic lakes and reservoirs and coastal waters when phytoplankton blooms occur.

This study focused on (a) determining the ability of the two- and three-band models to estimate chl-*a* concentrations below  $20 \text{ mg m}^{-3}$ , typical for estuarine and coastal case 2 waters, and (b) assessing the potential of MODIS and MERIS for estimating chl-*a* concentrations using red and near-infrared (NIR) bands. The results of this study were used for estimating chl-*a* concentrations in reservoirs of Dnieper River (Ukraine) as well as Don River and Azov Sea (Russia) using MODIS and MERIS data (Moses *et al* 2009).

## 2. Data and methods

From July through November 2008, 89 stations were sampled in the Fremont State Lakes in eastern Nebraska, USA. At each station Secchi disk depth was measured and water samples were collected at a depth of 0.5 m. A standard set of water quality variables was measured: turbidity and concentrations of chl-*a*, total, inorganic, and organic suspended solids (TSS, ISS, OSS, respectively).

Hyperspectral reflectance measurements were taken from a boat using two intercalibrated Ocean Optics USB2000 spectrometers each couples 2048-element linear CCD-array detector. Data were collected in the range of 400–900 nm with a sampling interval of 0.3 nm, a spectral resolution of 1.5 nm and signal to noise ratio of above 250. Radiometer 1, equipped with a 25° field-of-view optical fibre, was pointed downward to measure the below-surface upwelling radiance,  $L_{\text{up}}(\lambda)$ , at nadir. The tip of the optical fibre was kept just below the water surface by means of a 2 m long, hand-held dark blue

pole. To simultaneously measure incident irradiance  $E_{\text{inc}}(\lambda)$ , radiometer 2, connected to an optical fibre fitted with a cosine collector, was pointed upward and mounted on a 2.5 m mast.

To match the transfer functions of the radiometers, intercalibration of the instruments was accomplished by measuring simultaneously the upwelling radiance  $L_{\text{cal}}(\lambda)$  from a white Spectralon® reflectance standard (Labsphere, Inc., North Sutton, NH), with the reflectance  $R_{\text{cal}}(\lambda)$ , and the corresponding incident irradiance  $E_{\text{cal}}(\lambda)$ . The remote-sensing reflectance at nadir was computed as:

$$R_{\text{rs}}(\lambda) = \frac{L_{\text{up}}(\lambda)}{E_{\text{inc}}(\lambda)} \times \frac{E_{\text{cal}}(\lambda)}{L_{\text{cal}}(\lambda)} \times 100 \times R_{\text{cal}}(\lambda) \times \frac{t}{n^2} \times \frac{F(\lambda)}{\pi} \quad (3)$$

where  $t$  is the water-to-air transmittance (taken equal to 0.98 (Mobley 1994)),  $n$  is the refractive index of water relative to air taken equal to 1.33,  $\pi$  is used to transform the irradiance reflectance,  $R$ , into remote-sensing reflectance,  $R_{\text{rs}}$ , and  $F$  is wavelength-dependent correction factor (the so-called immersion factor) calculated following Ohde and Siegel (2003). The immersion factor has to be applied if the sensors are immersed in water; it accounts for the change in the sensor response due to the different refractive index of the intervening medium (i.e., water) in contact with the optics.

The critical issue with regard to the dual-fibre approach is that the transfer functions, which describe the relationship of the incident flux impinging on the sensor to the data numbers produced by both radiometers, should be identical. We studied the identity of the two radiometers used in this study and found that the difference between their transfer functions did not exceed 0.4% (Dall'Olmo and Gitelson 2005).

Measured reflectances were averaged in the spectral bands of MODIS (band 13: 662–672 nm, band 15: 743–753 nm) and MERIS (band 7: 660–670 nm, band 9: 703–713 nm, and band 10: 748–755.5 nm) to simulate reflectances in the respective satellite spectral bands.

## 3. Results and discussion

The waters sampled had chl-*a* concentrations and turbidity values that varied by a factor of about 10 (table 1). TSS and concentrations correlated weakly with chl-*a* (figure 1), confirming that the water bodies sampled belong to case 2 waters (Morel and Prieur 1977).

The remote-sensing reflectance was highly variable over the visible and NIR spectral regions (figure 2). The spectra were quite similar in magnitude and shape to reflectance spectra collected in turbid productive waters (Lee *et al* 1994, Gitelson *et al* 2000, Dall'Olmo and Gitelson 2005, Schalles 2006). The standard deviation of the reflectance had maximal values in the green and red spectral regions.

The maximum band ratio, calculated as maximum of three band ratios at wavelength 443, 490, 520 and 565 nm ( $R_{\text{rs}443}/R_{\text{rs}565}$ ,  $R_{\text{rs}490}/R_{\text{rs}565}$ ,  $R_{\text{rs}520}/R_{\text{rs}565}$ ), used for estimating chl-*a* concentrations in case I ocean waters (e.g., O'Reilly *et al* 1998), was poorly related to the chl-*a* concentrations (figure 3) due to multiple factors that contribute to the reflectance patterns in these spectral regions.

**Table 1.** Descriptive statistics of the optical water quality parameters measured.

		Min	Max	Median	Mean	STD <sup>a</sup>	CV <sup>b</sup>	N <sup>c</sup>
Chl- <i>a</i>	mg m <sup>-3</sup>	2.07	183.53	23.70	29.33	26.11	0.89	89
SD	m	0.51	4.20	0.98	1.21	0.70	0.58	89
Turbidity	NTU	1.51	19.20	6.79	7.59	4.39	0.58	89
TSS	mg l <sup>-1</sup>	1.19	15.00	6.80	7.30	3.26	0.45	89
ISS	mg l <sup>-1</sup>	0.15	5.85	0.80	1.11	0.95	0.86	87
OSS	mg l <sup>-1</sup>	0.81	12.80	6.00	6.26	2.97	0.47	87

<sup>a</sup> Standard deviation of water quality parameters.

<sup>b</sup> Coefficient of variation (STD/mean).

<sup>c</sup> Number of samples.

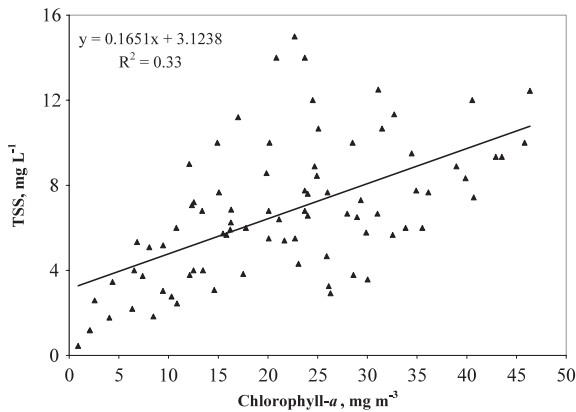


**Figure 1.** TSS concentrations versus chl-*a* concentrations.

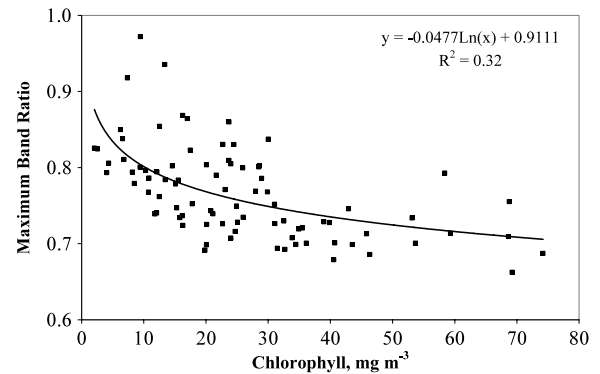


**Figure 3.** Maximum band ratio versus chl-*a* concentrations.

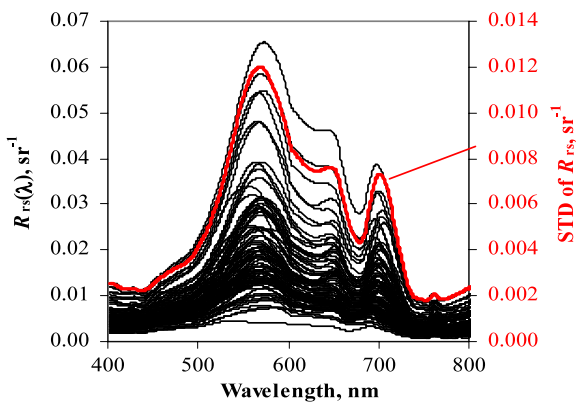


**Figure 2.** Remote-sensing reflectance,  $R_{rs}$ , spectra and spectrum of their standard deviation, STD (in red, right axis).

These include absorption by CDOM and NAP as well as backscattering by particulate matter. Thus, this algorithm was inadequate for accurately estimating chl-*a* concentrations in these case 2 waters.

Using an optimization procedure for the three-band model equation (2) (Dall’Olmo and Gitelson 2005), the optimal spectral region for  $\lambda_1$  was found around 670 nm, which is in accord with previous studies (Dall’Olmo and Gitelson 2005, Gitelson *et al* 2008).

However, the reciprocal reflectance at 670 nm,  $R_{670}^{-1} \propto (a + b_b)/b_b$ , was governed by other factors (i.e., TSS,

absorption by non-algal particles and CDOM) in addition to chl-*a*. Thus, despite an increase in absorption as chl-*a* increased, the relationship  $R_{670}^{-1}$  versus chl-*a* had a negative slope (figure 4(A)).  $R_{670}^{-1}$  was strongly affected by scattering by TSS, which increases with an increase in chl-*a* (figure 4(B)).

To reduce the effects of scattering by suspended particles and absorption by non-algal particles and CDOM,  $R^{-1}(\lambda_2)$  at 710 nm was used.  $R_{710}^{-1} \propto (a_{CDOM} + a_{nap} + a_{water} + b_b)/b_b$  was strongly related to TSS concentration (figure 4(B)) as well as to absorption by all materials except chl-*a*.

Thus, the difference  $R_{670}^{-1} - R_{710}^{-1} \propto a_{chl}/b_b$  was more closely related to chl-*a* than  $R_{670}^{-1}$  (figure 4(C)). However, it was still dependent on  $b_b$  and it was strongly affected (especially for chl-*a* < 10 mg m<sup>-3</sup>) by scattering by suspended particles.

The reflectance in the NIR range of the spectrum is closely related to  $b_b$ , so  $R_{750} \propto b_b$  was used to remove the effect of the differences between samples in scattering by suspended particles. Thus, the model (equation (2)) with  $\lambda_1 = 665\text{--}675$  nm,  $\lambda_2 = 705\text{--}715$  nm and  $\lambda_3 = 745\text{--}755$  nm was closely and almost linearly related to chl-*a* with an estimation error of < 1.65 mg m<sup>-3</sup> (figure 4(D)).

The same model (equation (2)) was used to assess the potential of MODIS and MERIS to retrieve the chl-*a* concentration in turbid productive waters.

We tested the model in the form

$$\text{MODIS}_{2\text{band}} = R_{15}/R_{13} \quad (4)$$

$$\text{MERIS}_{3\text{band}} = (R_7^{-1} - R_9^{-1}) \times R_{10} \quad (5)$$

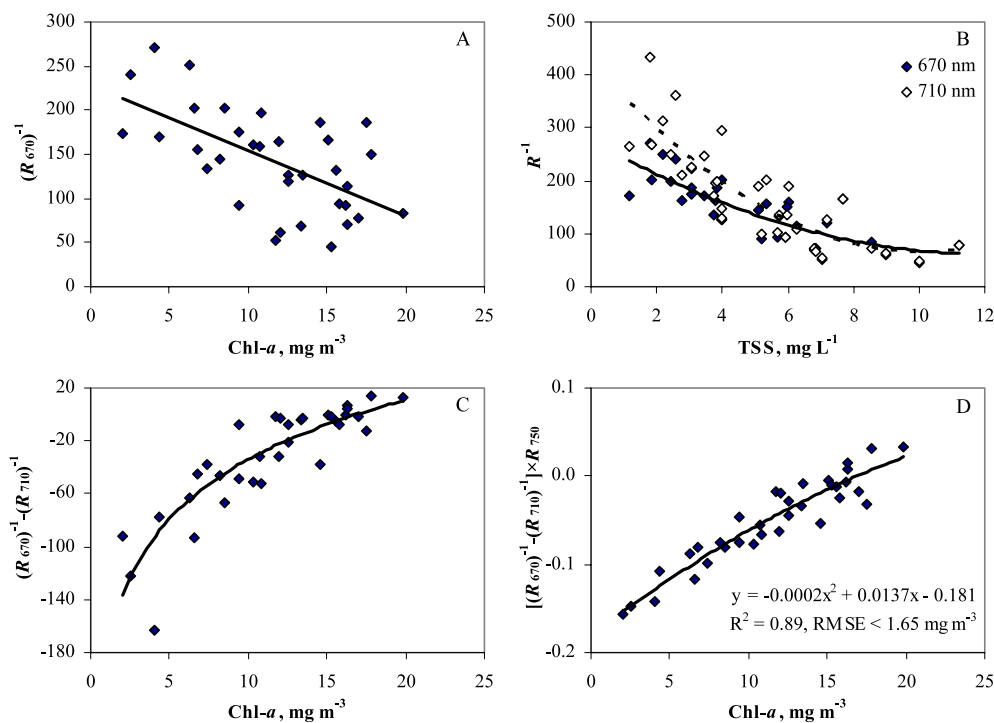


**Figure 4.** Reciprocal reflectances at 670 nm versus chl-*a* concentrations (A), reciprocal reflectances at 670 and 710 nm versus TSS concentrations (B), differences of reciprocal reflectances,  $(R_{670})^{-1} - (R_{710})^{-1}$  versus chl-*a* (C), and three-band model,  $[(R_{670})^{-1} - (R_{710})^{-1}] \times R_{750}$ , versus measured chl-*a* concentrations (D).

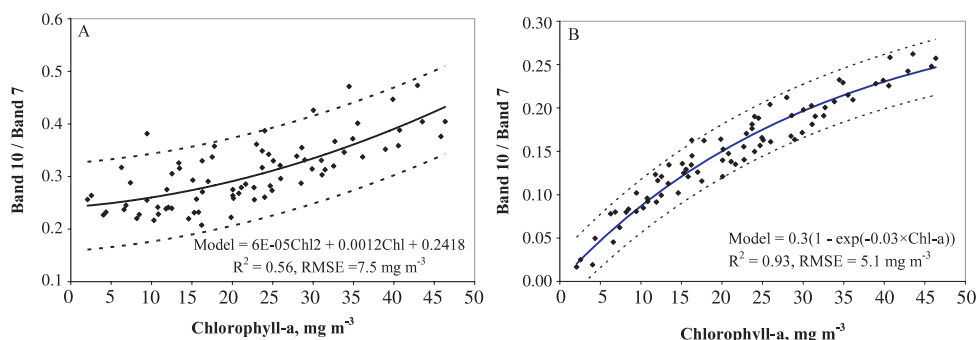


**Figure 5.** Two-band model values with simulated MODIS bands (A), and three-band model values with simulated MERIS bands (B), versus chl-*a* concentrations.

where  $R_i$  is the surface reflectance in band  $i$  of MODIS and MERIS.

The MODIS two-band model (equation (4)) was able to estimate chl-*a* ranging from 2 to 50  $\text{mg m}^{-3}$  with a RMSE < 7.5  $\text{mg m}^{-3}$ . However, the model was almost insensitive to chl-*a* < 20  $\text{mg m}^{-3}$  (figure 5(A)). The MERIS three-band model (equation (5)) was able to accurately estimate chl-*a* ranging from 2 to 50  $\text{mg m}^{-3}$  with RMSE < 5.1  $\text{mg m}^{-3}$  (figure 5(B)) and chl-*a* < 20  $\text{mg m}^{-3}$  with a RMSE < 1.7  $\text{mg m}^{-3}$ .

**4. Conclusions**

The results obtained in this study provide evidence that the three-band model which uses red and NIR bands is able to accurately estimate low to moderate chlorophyll-

*a* concentrations in turbid productive waters. With an accurate atmospheric correction of satellite data in the red and NIR spectral bands, the two-band model can be applied to MODIS data for estimating moderate-to-high chlorophyll-*a* concentrations exceeding 20  $\text{mg m}^{-3}$  (i.e., in phytoplankton bloom conditions). The existence of a spectral band at 708 nm provides a significant advantage for MERIS data. Benefiting from the higher spectral resolution of the MERIS data, both the two-band and three-band models can be reliably applied for estimating wide ranging chl-*a* concentrations including chl-*a* < 20  $\text{mg m}^{-3}$ , typical for coastal and estuarine waters.

**Acknowledgments**

This research was supported by NASA Land Use Land Cover Change Program grant NNG06GG17G to AG. A contribution

of the University of Nebraska Agricultural Research Division, Lincoln. This research was also supported in part by funds provided through the Hatch Act.

## References

- Dall'Olmo G and Gitelson A A 2005 Effect of bio-optical parameter variability on the remote estimation of chlorophyll-*a* concentration in turbid productive waters: experimental results *Appl. Opt.* **44** 412–22
- Dall'Olmo G and Gitelson A A 2006 Effect of bio-optical parameter variability and uncertainties in reflectance measurements on the remote estimation of chlorophyll-*a* concentration in turbid productive waters: modeling results *Appl. Opt.* **45** 3577–92
- Dall'Olmo G, Gitelson A A, Rundquist D C, Leavitt B, Barrow T and Holz J 2005 Assessing the potential of SeaWiFS and MODIS for estimating chlorophyll concentration in turbid productive waters using red and near-infrared bands *Remote Sens. Environ.* **96** 176–87
- Gitelson A 1992 The peak near 700 nm on reflectance spectra of algae and water: relationships of its magnitude and position with chlorophyll concentration *Int. J. Remote Sens.* **13** 3367–73
- Gitelson A, Keydan G and Shishkin V 1985 Inland waters quality assessment from satellite data in visible range of the spectrum *Sov. Remote Sens.* **6** 28–36
- Gitelson A A, Dall'Olmo G, Moses W, Rundquist D C, Barrow T, Fisher T R, Gurlin D and Holz J 2008 A simple semi-analytical model for remote estimation of chlorophyll-*a* in turbid waters: validation *Remote Sens. Environ.* **112** 3582–93
- Gitelson A A, Gritz U and Merzlyak M N 2003 Relationships between leaf chlorophyll content and spectral reflectance and algorithms for non-destructive chlorophyll assessment in higher plant leaves *J. Plant Physiol.* **160** 271–82
- Gitelson A A, Schalles J F and Hladik C M 2007 Remote chlorophyll-*a* retrieval in turbid, productive estuaries: Chesapeake Bay case study *Remote Sens. Environ.* **109** 464–72
- Gitelson A A, Viña A, Ciganda V, Rundquist D C and Arkebauer T J 2005 Remote estimation of canopy chlorophyll content in crops *Geophys. Res. Lett.* **32** L08403
- Gitelson A A, Yacobi Y Z, Schalles J F, Rundquist D C, Han L, Stark R and Etzion D 2000 Remote estimation of phytoplankton density in productive waters *Arch. Hydrobiol.* **55** 121–36
- GKSS 1986 The use of chlorophyll fluorescence measurements from space for separating constituents of sea water *ESA Contract No. RFQ3-5059/84/NL/MD* vol II, GKSS Research Centre, Germany
- Gons H J 1999 Optical teledetection of chlorophyll *a* in turbid inland waters *Environ. Sci. Technol.* **33** 1127–32
- Gordon H and Morel A 1983 Remote assessment of ocean color for interpretation of satellite visible imagery. A review *Lecture notes on Coastal and Estuarine Studies* vol 4 (Berlin: Springer)
- Gordon H R, Brown O B, Evans R H, Brown J W, Smith R C, Baker K S and Clark D K 1988 A semianalytic radiance model of ocean color *J. Geophys. Res.* **93** 10909–24
- Gower J F R, Doerffer R and Borstad G A 1999 Interpretation of the 685 nm peak in water-leaving radiance spectra in terms of fluorescence, absorption and scattering, and its observation by MERIS *Int. J. Remote Sens.* **20** 1771–86
- Lee Z P, Carder K L, Hawes S K, Steward R G, Peacock T G and Davis C O 1994 Model for the interpretation of hyper-spectral remote-sensing reflectance *Appl. Opt.* **33** 5721–32
- Mobley C D 1994 *Light and Water: Radiative Transfer in Natural Waters* (San Diego, CA: Academic)
- Morel A and Prieur L 1977 Analysis of variations in ocean color *Limnol. Oceanogr.* **22** 709–22
- Moses W J, Gitelson A A, Berdnikov S and Povazhnyy V 2009 Estimation of chlorophyll-*a* concentration in case II waters using MODIS and MERIS data—successes and challenges *Environ. Res. Lett.* **4** 045005
- Ohde T and Siegel H 2003 Derivation of immersion factors for the hyperspectral Trios radiance sensor *J. Opt. A: Pure Appl. Opt.* **5** 12–4
- O'Reilly J E, Maritorena S, Mitchell B G, Siegel D A, Carder K L and Garver S A 1998 Ocean color chlorophyll algorithms for SeaWiFS *J. Geophys. Res.* **103** 24937–53
- Schalles J F 2006 Optical remote sensing techniques to estimate phytoplankton chlorophyll-*a* concentrations in coastal waters with varying suspended matter and CDOM concentrations *Remote Sensing of Aquatic Coastal Ecosystem Processes: Science and Management Applications* ed L Richardson and E Ledrew (Berlin: Springer) pp 27–79
- Stumpf R P and Tyler M A 1988 Satellite detection of bloom and pigment distributions in estuaries *Remote Sens. Environ.* **24** 385–404
- Vasilkov A and Kopelevich O 1982 Reasons for the appearance of the maximum near 700 nm in the radiance spectrum emitted by the ocean layer *Oceanology* **22** 697–701